6964 J. Med. Chem. 2010, 53, 6964–6972
DOI: 10.1021/jm100581z

Journal of Medicinal Chemistry Article

In Vitro and in Vivo Trypanocidal Evaluation of Nickel Complexes with an Azapurine Derivative against *Trypanosoma cruzi*

Carmen R. Maldonado,[†] Clotilde Marín,[‡] Francisco Olmo,[‡] Oscar Huertas,[‡] Miguel Quirós,[†] Manuel Sánchez-Moreno,[‡] María J. Rosales,[‡] and Juan M. Salas*,[†]

[†]*Department of Inorganic Chemistry and* [‡]*Department of Parasitology, University of Granada, 18071 Granada, Spain*

Received May 12, 2010

Seven ternary nickel(II) complexes (three previously described and four firstly described here) with an azapurine derivative (the anionic form of 4,6-dimethyl-1,2,3-triazolo[4,5-*d*]pyrimidin-5,7-dione) have been synthesized and spectroscopically characterized, and the crystal structures of three of them have been solved by X-ray diffraction. Studies in vitro and in vivo on the antiproliferative activity of these complexes against *Trypanosoma cruzi* (epimastigote, amastigote, and trypomastigote forms) have been carried out, displaying in some cases significantly higher antitrypanosomatid activity and lower toxicity than the reference drug for Chagas' disease, benznidazole (*N*-benzyl-2-(2-nitro-1*H*-imidazol-1-yl)-acetamide). Ultrastructural analysis and metabolism excretion studies were also executed in order to propose a possible mechanism of action for the assayed drugs.

1. Introduction

Chagas' disease, caused by the protozoan *Trypanosoma cruzi*, is a neglected disease that affects 12−14 million people in areas of endemicity in Latin America, where approximately 100 million people are at risk.[1] The disease is a major public health problem in the affected areas. The infection triggers an important cardiomyopathy for which the pathophysiological mechanisms are not completely understood.[2,3] Current chemotherapy is based largely on nifurtimox ((*RS*)-3-methyl-*N*-[(1*E*)-(5-nitro-2-furyl)methylene]thiomorpholin-4-amine 1,1-dioxide) and benznidazole (BZN,[a] *N*-benzyl-2-(2-nitro-1*H*-imidazol-1-yl)acetamide; see Scheme 1), which are only partially effective and have considerable side effects.[4,5] Both drugs are active in the acute phase of the disease, but their efficacies are very low in the established chronic phase. Moreover, differences in drug susceptibility among different *T. cruzi* strains lead to varied parasitological cure rates according to the geographical area. Extensive work in the past 2 decades has helped to understand the molecular basis of the antichagasic activity of both drugs.[6] Most frequent side effects of these drugs include anorexia, vomiting, peripheral polyneuropathy, and allergic dermopathy. These effects are probably a result of oxidative or reductive damage to the host's tissue and are thus inextricably linked to their antiparasitic activity.[7] For all these reasons, there is urgent need for new drugs.

For the development of more effective and reliable agents, a large number of compounds bearing nitrogen-containing fused heterocyclic skeletons, such as 4-anilinoquinazolines, pyrazolopyrimidines, triazolopyrimidines, pyrrolopyrimidines, pyrazolopyridazines, and imidazopyrazines, have been discovered, and many of them exhibit excellent anticancer, antimicrobial, and antiprotozoal activity.[8−10] Examples of compounds that have shown activity against *T. cruzi* and have been clinically tested are itraconazole, posaconazole, and different biphosphonates.[11]

Recently, 1,2,4-triazolo[1,5-*a*]pyrimidines, which may be considered as mimetics of purines, have attracted increasing attention because of their potential biological activity, mainly against parasites, with promising first results.[12,13] Following this line, we have started to explore the coordination possibilities of another triazolopyrimidine family: 1,2,3-triazolo[4,5-*d*]-pyrimidines which possess three contiguous N atoms in the imidazole ring and may also be regarded as purine derivatives, replacing the C2 atom of the imidazole ring with a N atom. For this reason, these compounds may also be named as 8-azapurines, using a biochemical instead of a systematic IUPAC nomenclature and numbering scheme (see Scheme 2). The 1,2,3-triazolo[4,5-*d*]pyrimidine family includes, among others, several derivatives with amino and/or hydroxyl substitutes in positions 5 and 7, which may be named using the biochemical nomenclature as 8-azaadenines, 8-azaguanines, 8-azaxanthines, and 8-azahypoxanthines. Some reported studies warn of the potential biological applications (antiviral activity, inhibition of cyclin-dependent kinases, affinity for A1 adenosine receptors) of these derivatives,[14−16] but nevertheless, the interaction of transition metal ions with 1,2,3-triazolo[4,5-*d*]pyrimidines has been the subject of relatively few chemical, spectroscopic, and crystallographic studies, which contrasts with the large amount of data accumulated for purines.

In view of the above findings and as a continuation of our effort to identify new candidates that are potent, selective, and

*To whom correspondence should be addressed. Address: Departamento de Química Inorgánica, Facultad de Ciencias. Av. Fuentenueva s/n, 18071, Granada, Spain. Phone: +34 958248525. Fax: +34 958248526. E-mail: jsalas@ugr.es.

[a] Abbreviations: BZN, benznidazole; TEM, transmission electronic microscopy; DSC, differential scanning calorimetry; TG, thermogravimetry; en, ethylenediamine; dap, 1,3-diaminopropane; bapa, bis(3-aminopropyl)amine; phen, 1,10-phenanthroline; bpy, 2,2′-bipyridyl; dpyamin, 2,2′-dipyridylamine; IC_{50}, concentration required for 50% inhibition; IC_{25}, concentration required for 25% inhibition; SI, selectivity index; DMSO, dimethylsulfoxide; p.i., postinfection.

 Published on Web 09/02/2010

Scheme 1. Drugs Currently Used against Chagas' Disease

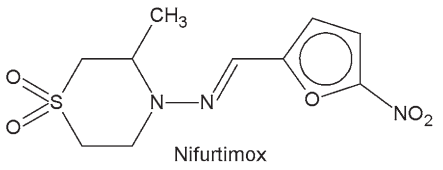

Nifurtimox

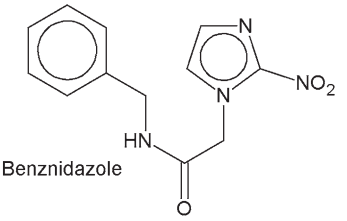

Benznidazole

Scheme 2. Purine and 1,2,3-Triazolo[4,5-*d*]pyrimidine Skeletons Displaying the Biochemical and IUPAC Numbering Schemes, Respectively, and the Molecular Structure of Hdmax, the Main Ligand in This Work

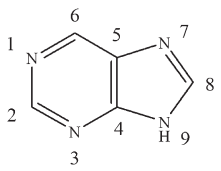

Purines

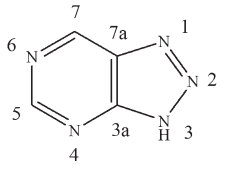

1,2,3-triazolo-[4,5-*d*]pyrimidines (8-azapurines)

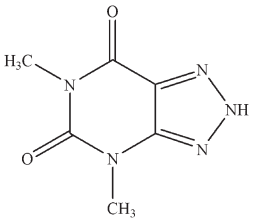

4,6-dimethyl-1,2,3-triazolo-[4,5-*d*]pyrimidin-5,7-dione (Hdmax)

less toxic antitrypanosomatids, we report here the synthesis and structural characterization of seven nickel(II) complexes (four of them new, three previously described) bearing the anionic form of 4,6-dimethyl-1,2,3-triazolo[4,5-*d*]pyrimidin-5,7-dione (Hdmax, **1**, see Scheme 2), which have been synthesized, spectroscopically characterized, and examined for antiproliferative in vitro and in vivo activity against *T. cruzi* (epimastigote, amastigote, and trypomastigote forms). Unspecific mammal cytotoxicity of the most active compounds was evaluated in vitro, and the less toxic derivatives were submitted in vivo for a more thorough study. Furthermore, we also include a NMR study concerning the nature and percentage of the excretion metabolites in order to get some information about the inhibitory effect of our compounds over the glycolytic pathway, since it represents the prime source of energy for the parasite. Finally, the effect of compounds on the ultrastructure of *T. cruzi* was considered on the basis of transmission electronic microscopy (TEM) experiments.

2. Results and Discussion

2.1. Chemistry. The compounds assayed were nickel(II) complexes bearing the anionic form of 4,6-dimethyl-1,2,3-triazolo[4,5-*d*]pyrimidin-5,7-dione, dmax (also known as 1,3-dimethyl-8-azaxanthine), and different aliphatic amines [ethylenediamine (en), 1,3-diaminopropane (dap), bis(3-aminopropil)amine (bapa)] or aromatic amines [1,10-phenanthroline (phen), 2,2′-bipyridyl (bpy), 2,2′-dipyridylamine (dpyamin)] as auxiliary ligand (see Experimental Section). The free triazolopyrimidine derivative (**1**) and its nickel salt (**2**) have also been tested in order to compare their activity (IC_{50}) with that of the ternary nickel complexes.

The triazolopyrimidine derivative (**1**), the corresponding nickel salt (**2**), and those complexes containing an aliphatic amine in their structures (**3**, **4**, and **5**, see section 4.1) have been previously described and characterized by us.[17,18] The remaining four compounds (**6**, **7**, **8**, and **9**) are novel. These four nickel compounds have been characterized by elemental analysis, infrared spectroscopy, thermal studies, diffuse reflectance spectroscopy and magnetic measurements. Furthermore, the crystal structures of three of them have been solved by single crystal X-ray diffraction (see Table 1).

The IR spectra of the compounds were measured in the region 4000−400 cm^{-1} showing the characteristic bands of both ligands, the anionic form of the triazolopyrimidine ligand (dmax) and the corresponding aromatic amine. The 1700−1500 cm^{-1} region of the infrared spectra of the free heterocycle (**1**) displays three bands at 1717, 1681, and 1604 cm^{-1}, assignable to carbonyl stretching and possibly to $\delta(H_2O)$, these bands being slightly displaced to lower (the first two) or higher (the last one) wavenumbers in the complexes. For all the complexes, a new band appears at 1544 cm^{-1}, characteristic of the anionic form of this ligand,[17] and an intense band close to 1310 cm^{-1} is present in the region expected for vibrational modes of the aromatic ring. The spectra also show broad bands in the 3500−3300 cm^{-1} region, assignable to ν(OH) of water, broadened and lower wavenumber displaced by the hydrogen bonds, and defined bands in the 3100−2900 cm^{-1} region, assignable to ν(CH) of aromatic groups.

The first step of the thermal decomposition of the isolated complexes (except for **6** that is anhydrous) is their dehydration. This process is responsible for a well-defined weight loss effect in the TG diagram which agrees well with the elimination of the water molecules indicated by elemental analysis; the endothermic effect in the DSC diagram begins at room temperature, making it impossible to calculate the dehydration enthalpies. The most interesting feature of the thermal analysis of compounds **8** and **9** is perhaps the endothermic elimination of one molecule of the auxiliary ligand separately from the pyrolysis of the sample. This process is responsible for the endothermic peaks at 308 and 321 °C for **8** and 300 °C for **9** which are separated enough from the exothermic effects of pyrolytic decomposition to calculate the enthalpy of this elimination: ΔH of 63.9 and 58.5 kJ/mol auxiliary ligand, respectively. Finally, the pyrolytic decomposition of the organic moiety for the four compounds gives the corresponding nickel oxide as inorganic residue.

The electronic spectra for the nickel compounds show two of the three typical bands expected for octahedral Ni(II) complexes ($^3T_{2g}(F) \leftarrow {}^3A_{2g}(F)$, ν_1, and $^3T_{1g} \leftarrow {}^3A_{2g}(F)$, ν_2). These bands appear at 11 587 and 18 727 cm^{-1} (**6**), 12 516 and 19 157 cm^{-1} (**7**), 11 455 and 18 797 cm^{-1} (**8**), and 11 325 and 17 857 cm^{-1} (**9**). The parameters 10 Dq (11 587, 12 516, 11 455,

Table 1. Crystal Data

parameter	6	7	8
chemical formula	$C_{36}H_{28}N_{14}NiO_4$	$C_{48}H_{50}N_{16}NiO_{11}$	$C_{32}H_{28}N_{14}NiO_4$
formula weight	779.43	1085.75	731.39
crystal size	0.22 mm × 0.19 mm × 0.07 mm	0.48 mm × 0.44 mm × 0.42 mm	0.15 mm × 0.11 mm × 0.02 mm
crystal system	monoclinic	triclinic	triclinic
space group	$C2/c$	$P\bar{1}$	$P\bar{1}$
unit cell dimensions			
a (Å)	13.226(3)	13.8735(16)	8.738(2)
b (Å)	15.714(3)	14.2569(16)	12.350(3)
c (Å)	16.609(3)	15.0005(17)	16.754(4)
α (deg)	90	106.463(2)	73.779(6)
β (deg)	90.107(4)	99.654(2)	75.733(5)
γ (deg)	90	113.031(2)	69.310(4)
volume (Å^3)	3451.8(11)	2484.7(5)	1601.9(7)
Z	4	2	2
density (calcd, g/cm^3)	1.500	1.451	1.516
absorption coefficient (mm^{-1})	0.626	0.469	0.669
θ range for data collection (deg)	2.01−28.34	1.49−28.29	1.80−28.17
reflections collected/unique	20042/4080	29148/11246	10086/6890
data/restraints/parameters	4080/0/251	11246/6/716	6890/0/464
goodness of fit on F^2	0.877	0.962	0.707
R ($I \geq 2\sigma(I)$)	0.0435	0.0497	0.0587
wR^2 (all data)	0.1000	0.1529	0.1187
largest diff peak and hole (e·Å^{-3})	0.349, −0.176	0.700, −0.314	0.451, −0.336

and 11 325 cm^{-1}, respectively) and B (994, 771, 1105, and 826 cm^{-1}, respectively) were calculated using Dou's equations.[19] For $[Ni(phen)_3]^{2+}$ (**7**) the values for the bands are similar to those found in the literature for $[Ni(bpy)_3]^{2+}$,[20] while for the rest of compounds these values are close to others nickel complexes with triazolopyrimidine derivatives.[18,21]

The magnetic susceptibility of the nickel complexes has been measured in the 2−300 K range, all samples behaving as magnetically diluted compounds with small or negligible and probably unspecific magnetic interactions. The experimental data have been fitted to the Curie−Weiss law.[22] From the Curie constant, the value for the effective magnetic moment at $T \rightarrow \infty$ has been calculated yielding values 3.00−3.07 μ_B, and θ is close to zero in all cases, ranging from −0.13 to 0.42 K (compounds **7** and **6**, respectively).

2.2. X-ray Studies. Four of the tested nickel(II) complexes have been obtained as crystals suitable for monocrystal X-ray analysis, and their crystal structures have been determined. The crystallographic data for **3** have been previously published by us.[18] For the remaining three, the analysis of their crystal structures is described here. For **7**, only the phenanthroline ligands are directly linked to the metal ion, building the well-known cationic complex $[Ni(phen)_3]^{2+}$, with two triazolopyrimidinato anions (dmax) acting as noncoordinated counteranions and seven interstitial water molecules; whereas for **6** and **8** both ligands are directly bonded to the metal center building the neutral complexes $[Ni(dmax)_2(L)_2]$ (L = phen, bpy), with the triazolopyrimidine ligand linked through the less-hindered triazole nitrogen atom (N2), which is the binding site observed in previously reported azaxanthinato complexes.[21] Despite their similar molecular structures, compounds **6** and **8** are not isostructural. The auxiliary ligands are coordinated as usual through their two nitrogen ligands forming five-membered chelate rings. The molecular units of these three nickel complexes are shown in Figure 1.

In the three complexes, the coordination polyhedron is a fairly regular octahedron with Ni−N distances ranging from 2.0749(19) to 2.1086(18) Å, from 2.064(2) to 2.120(2) Å, and from 2.080(4) to 2.121(4) Å for **7**, **6**, and **8**, respectively. For **7**, the geometrical parameters are identical to those found in the literature for other complexes containing the cationic species $[Ni(phen)_3]^{2+}$.[23,24] The ionization of the acidic proton of **1**, located at N2 in the crystal structure of the free ligand,[25] leads to the closure of the endocyclic angle at N2 (4.1−4.4°, 4.0°, 3.7−4.5°) and the opening of the adjacent endocyclic angles at N1 (3.0−3.5°, 3.0°, 1.7−2.9°) and N3 (3.7−2.5°, 2.9°, 3.8−2.3°), respectively, but the differences with the free ligand are slightly smaller when the triazolopyrimidinato is coordinated to the nickel center, showing that the effect of the loss of the proton is partially compensated by the presence of the metal cation. Otherwise, the differences in the equivalent distances between the free heterocycle and the deprotonated form at N2 are lower than 0.04 Å.

The presence of a large number of water molecules together with the capacity of this triazolopyrimidine to establish hydrogen bonds creates a very wide and complex hydrogen-bond network in **7**. On the other hand, in **6** and **8** only weak and rather unspecific intermolecular interactions take place.

2.3. In Vitro Antitrypanosomatid Activity. The inhibitory effect on the in vitro growth of *T. cruzi* epimastigote of the seven ternary nickel complexes, the azapurine derivative (**1**), and its nickel salt (**2**) was measured at different times, following established procedures (see Experimental Section). The ability of the compounds to inhibit the growth of the epimastigote forms was evaluated at 1, 10, 25, 50, and 100 μM, and the IC_{50} was determined for the most active compounds, where benznidazole (BZN) was used as reference drug. The results, including toxicity values against Vero cells, are displayed in Table 2. After 72 h of exposure, two of the nickel complexes showed IC_{50} values significantly lower than that for the reference drug (**8** and **6** with $IC_{50} < 1$ μM) while the results for other four are very close to that of BZN ($IC_{50} = 15$ μM for **9**, **4**, **7** and $IC_{50} = 30$ μM for **3**). On the other hand, the triazolopyrimidine ligand (**1**), its nickel salt (**2**), and the remaining ternary nickel complex (**5**) have IC_{50} much higher than BZN (16 μM).

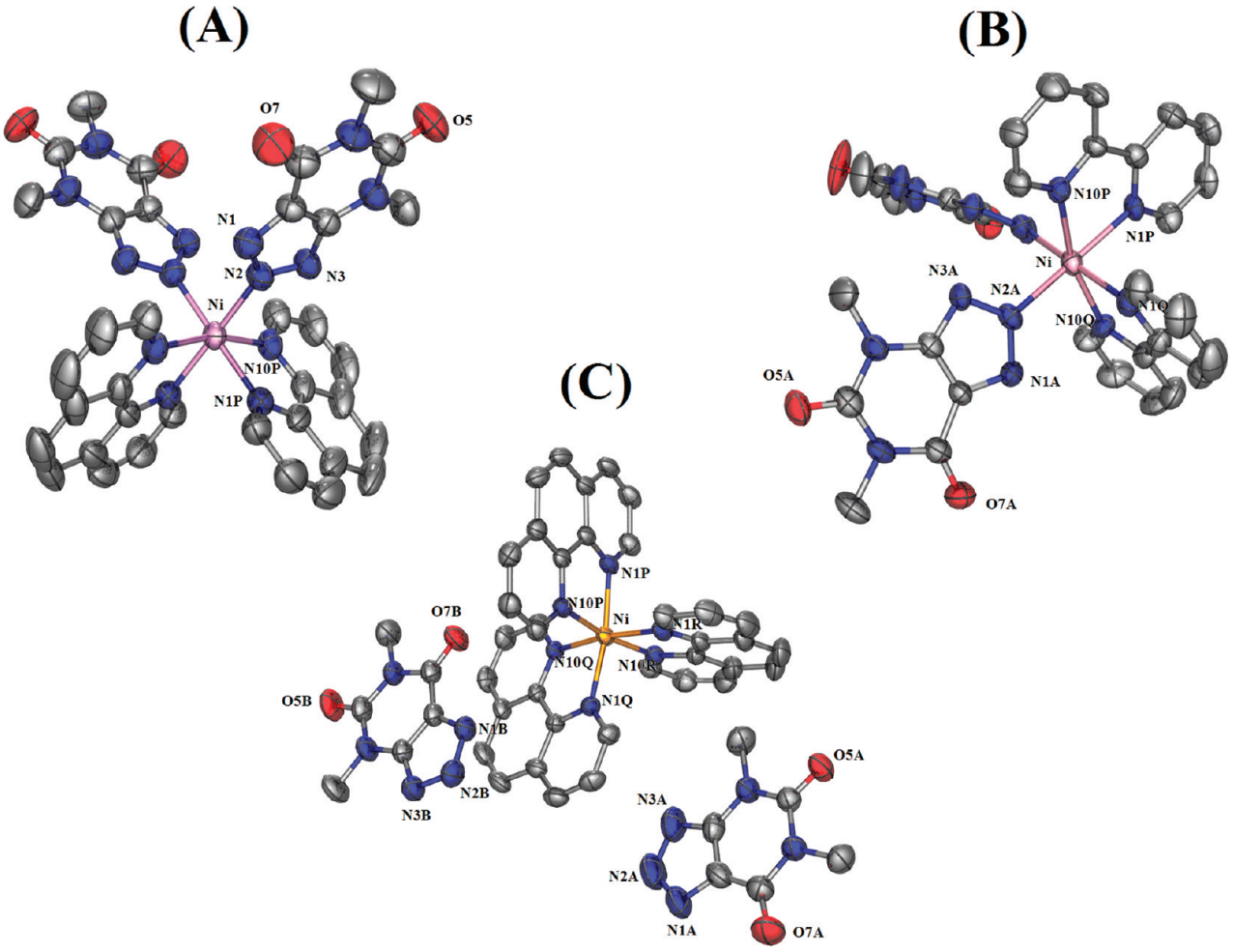

Figure 1. X-ray structures and atom numbering schemes for complexes (A) $[Ni(dmax)_2(phen)_2]$ (**6**), (B) $[Ni(dmax)_2(bpy)_2](H_2O)_{0.5}$ (**8**), and (C) $[Ni(phen)_3](dmax)_2 \cdot 7H_2O$ (**7**). Hydrogen atoms and noncoordinated water molecules have been omitted for clarity.

Table 2. In Vitro Activity of the Assayed Compounds against *Trypanosoma cruzi*

	IC_{50} (μM)[a]		
compd	*T. cruzi*	toxicity	SI[b]
benznidazole	16	14	1
1	90	59	0.7
2	76	144	2
3	30	380	13
4	15	84	6
5	55	35	0.7
8	< 1	200	> 200
6	< 1	120	> 120
7	15	172	11
9	15	97	7

[a] On Vero cells and *T. cruzi* after 72 h of culture. IC_{50} = the concentration required to give 50% inhibition, calculated by linear regression analysis from the K_c values at concentrations employed (1, 10, 25, 50, and 100 μM). [b] Selectivity index = IC_{50}(Vero cells)/IC_{50}(epimastigote). Average of three separate determinations.

2.4. Unspecific Cytotoxicity. Cytotoxicity of these compounds, against mammalian cells, was also evaluated in vitro at 1, 10, 25, 50, and 100 μM, using Vero cells as the cellular model[26] (see Table 2). BNZ was included again as a reference drug. **8** and **6** showed the best selectivity indexes (SI = IC_{50}(Vero cells)/IC_{50}(epimastigote)), being more than 200 and 120 times less toxic than BNZ, respectively. Besides, the other four active ternary nickel complexes (**3**, **7**, **9**, and **4**) were much less toxic than the reference drug with SI values of 13, 11, 7, and 6, respectively (the value for BZN is below 1), while the rest of assayed compounds do not show good SI values. Only **5** showed a SI value lower than BZN, and this compound was eliminated from further assays.

2.5. Cell Assay. In most studies on activity assays of new compounds against parasites, parasitic forms that develop in vectors are used (epimastigotes in the case of *T. cruzi*) because of the ease of working with these forms in vitro. However, in this study, we have also included the effect of these compounds on the parasitic forms that are developed in the host (amastigotes and trypomastigotes), the study of which is of great importance, given that the final aim is to determine the effects in the definitive host.[13]

An experimental model designed in our laboratory has been used to predict the effect of those ternary nickel complexes, that have shown an important inhibition in vitro and a higher SI over the growth of extracellular forms, over the capacity of infection and growth of the intracellular forms and subsequent transformation to bloodstream forms of *T. cruzi*. Adherent Vero cells (1×10^5 Vero cells) were incubated for 2 days and then were infected with 1×10^6 metacyclic forms for 6 h (control experiment, Figure 2A). Afterward, the nonphagocytized parasites were removed and the culture kept in fresh medium for 10 days. The parasites invaded the cells and underwent morphological conversion to amastigotes within 1 day after infection. On day 10, the rate of

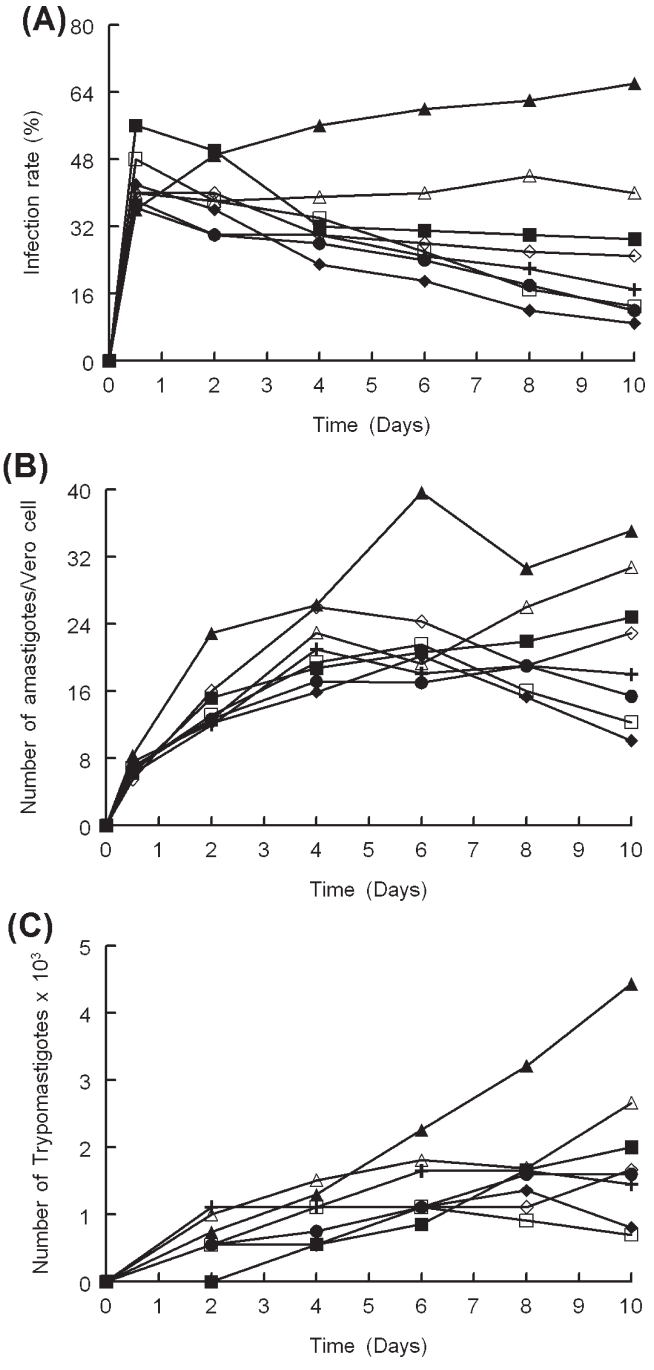

Figure 2. Effect of activity of the nickel(II) complexes on the infection rate and *T. cruzi* growth: (A) rate of infection; (B) mean number of amastigotes per infected Vero cell; (C) number of trypomastigotes in the culture medium; control (▲); BZN (△); **3** (●); **4** (+); **8** (◆); **6** (□); **7** (◇); **9** (■) (at IC_{25} concentration). The values are averages of three separate experiments.

host-cell infection reaches its maximum. When the drugs (IC_{25} concentration) were added simultaneously to Vero cells with *T. cruzi* metacyclic forms in exponential growth phase for 6 h, the infection rate significantly decreased with respect to the control in the order **8** > **3** ≥ **6** > **4** > **7** > **9**, with percentages of inhibition of infection capacity of 86%, 82%, 80%, 74%, 62%, and 56%, respectively. These values are remarkably higher than the inhibition achieved by BNZ (39%). In the control experiment, the average number of amastigotes per infected cell increased to 39.6 amastigotes/cell on day 6, decreasing to 30.6 amastigotes/cell on day 8, and increasing again until 35 amastigotes/cell on day 10 (see Figure 2B); these oscillations, in the number of amastigote forms per cell, are due to the parasite life cycle. When a cell is completely invaded of amastigote forms, the parasites break the cell; the breakage of the Vero cells implies the releasing and subsequent transformation of amastigotes into trypomastigotes. After that, trypomastigote forms can infect new cells in which they multiply, increasing the number of amastigotes per cell again. The six ternary nickel complexes inhibited *T. cruzi* amastigote replication in Vero cells in vitro, in a similar way as they inhibit the infection rate and again more efficiently than the reference drug. In the control experiment, the number of trypomastigotes in culture medium was 4.4×10^3 on day 10 postinfection (Figure 2C). The six tested compounds show a very significant decrease in number of trypomastigotes in media (84, 82, 67, 64, 62 and 55% for **6**, **8**, **4**, **3**, **7**, **9**, respectively), also higher than for the reference drug (BZN produces a 40% decrease).

2.6. In Vivo Anti *Trypanosoma cruzi* Evaluation. Because of the trypanocidal effect in vitro of these six triazolopyrimidine nickel complexes, we performed in vivo studies to evaluate the activity of them against *T. cruzi* infection in mice. Previously results had shown that the intravenous doping route resulted in high mortality rates;[28] for this reason, in this study we opted for the intraperitoneal route, using 5 mg/kg, which did not result in any animal mortality (data no shown). Female Swiss mice were inoculated intraperitoneally with 3000 blood trypomastigotes, and treatment began 7 days postinfection, with i.p. route of 1 mg/kg per day of each tested compound during 5 days. The administration was done using a saline solution. A group was treated in the same way with the vehicle (control). The level of parasitemia was determined every 2 days (Figure 3), the mortality was observed daily, and serological tests were performed 60 and 90 days postinfection (Table 3). None of the animals treated with the drugs nor the control died during the treatment, while in the groups of animals treated with BNZ the survival fraction was 80%. The six compounds were able to decrease the trypomastigote forms in the day that the experiment reached the maximum parasitic charge (day 25 postinfection) if compared with the positive control. In the groups of animals treated with the drugs (only one drug was tested in each group), a significant decrease of the parasitemia in day 40 postinfection was observed. The percentage of this decrease, with respect to the control, was in the range 89−47% for the nickel complexes and 9% for BZN. In fact, the levels of parasitemia observed for the assayed compounds were in agreement with their in vitro behavior, the in vivo activity varying, in general, in the order **8** > **3** ≥ **6** > **7** > **4** > **9**. None of the animals treated with the drugs that we had tested in our study or BZN, used as control in the antibodies studies, showed negative anti *T. cruzi* serology. However, all the compounds tested decreased antibodies levels between day 60 and day 90 (Table 3), showing higher performance than BZN in this assay. Differences in the level of anti *T. cruzi* antibodies are in agreement with the parasitemia findings. Although these compounds did not completely eliminate the circulating bloodstream trypomastigote forms, the number of them is substantially reduced. However, it cannot be expected that this decrease is going to protect against the damages associated with the chronic stage of the disease.[29]

2.7. Mechanism of Action Studies. Finally and in order to confirm or exclude some possible mechanisms of action, the

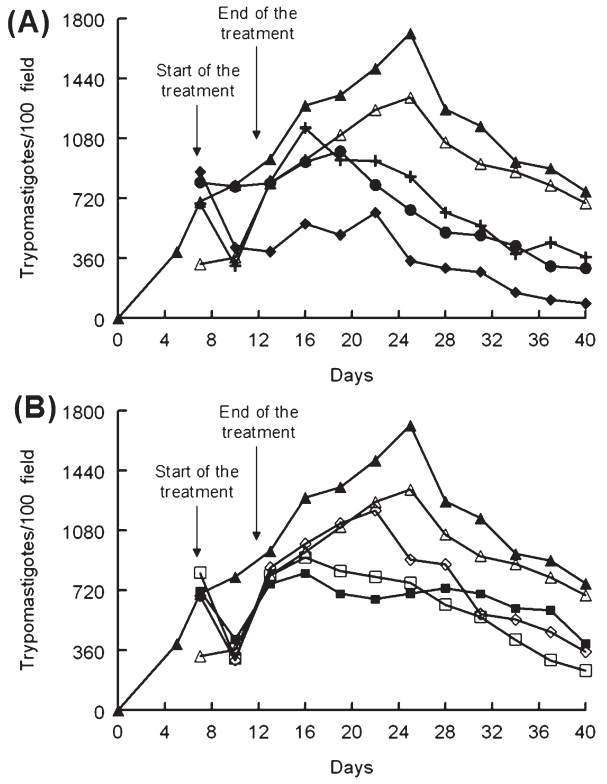

Figure 3. Parasitemia in the murine model of acute Chagas disease: (A) control (▲) and dose receiving 5 mg/kg BZN (△), **3** (●), **4** (+), and **8** (◆); (B) control (▲) and dose receiving 5 mg/kg BZN (△), **6** (□), **7** (◇), and **9** (■).

Table 3. Differences in the Level of Anti-*T. cruzi* Antibodies Expressed in Absorbance Units (AU) between Days 60 and 90 Postinfection for the Six Studied Compounds

treatment[b]	ΔA [a]
control (untreated)	0.1190
BZN	0.1160
3	−0.0813
4	0.1086
8	−0.0123
6	−0.0765
7	0.0234
9	0.0830

[a] 1 mg/kg per day, intraperitoneal route, administered during 5 days (see Experimental Section). [b] ΔA = (absorbance at 490 nm, day 90 p.i.) − (absorbance at 490 nm, day 60 p.i.).

effect on the energy metabolism and the changes of the parasite structure were studied.

2.7.1. Metabolite Excretion Effect. As far as it is known to date, none of the studied trypanosomatids are capable of completely degrading glucose to CO_2 under aerobic conditions, excreting into the medium a great part of their carbon skeleton as fermented metabolites, with variations depending on the considered species.[30] *T. cruzi* consumes glucose at a high rate, thereby acidifying the culture medium because of incomplete oxidation to acids. ^{1}H NMR spectra enabled us to determine the fermented metabolites excreted by the trypanosomatids during their in vitro culture. Figure 4B presents the spectrum given by cell-free medium 4 days after inoculation with the *T. cruzi* strain. Additional peaks, corresponding to the major metabolites produced and excreted during growth, were detected when this spectrum (Figure 4B) was compared with the one made with fresh

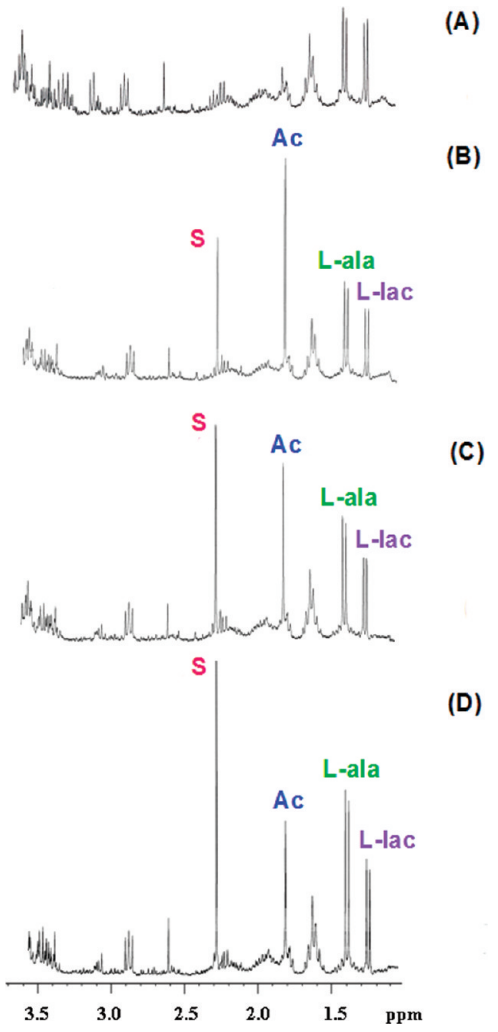

Figure 4. ^{1}H NMR spectra of epimastigote forms of *T. cruzi* treated with nickel(II) complexes (at IC_{25} concentration): (A) fresh medium; (B) control (untreated); (C) **3**; (D) **9**; (S) succinate; (Ac) acetate; (L-ala) L-alanine; (L-lac) L-lactate.

medium (Figura 4A). As shown, *T. cruzi* excretes acetate and succinate as major metabolites and L-alanine at a lower extent, data that agree well with other previously reported.[30,31] We used ^{1}H NMR for the identification and evaluation of the inhibiting effect caused by the compounds (**8**, **3**, **6**, **7**, **4**, and **9**) on metabolites excreted by *T. cruzi*. When the trypanosomatids were treated with **3** and **9**, the excretion of some of these catabolites (mainly acetate) was clearly disturbed (Figure 4C and Figure 4D, respectively) at the dosages assayed (IC_{25}). The role of acetate is probably to maintain the glycosomal redox balance. The inhibition of acetate excretion explains the observed increase in succinate, L-alanine, and L-lactate production, probably due to the action of these compounds at the pyruvate dehydrogenase complex level or to their disturbance of the mitochondria and, consequently, of the oxidative phosphorylation. BZN and the rest of the tested compounds did not produce any alteration in the energetic metabolism of the parasites (spectra not shown).

2.7.2. Ultrastructural Alterations Effect. Ultrastructural alterations in epimastigote forms of *T. cruzi* treated with these triazolopyrimidine complexes were observed (Figure 5). **3** and **4** were less effective (panel 2 of Figure 5 and panel 3 of Figure 5, respectively), most parasites showing

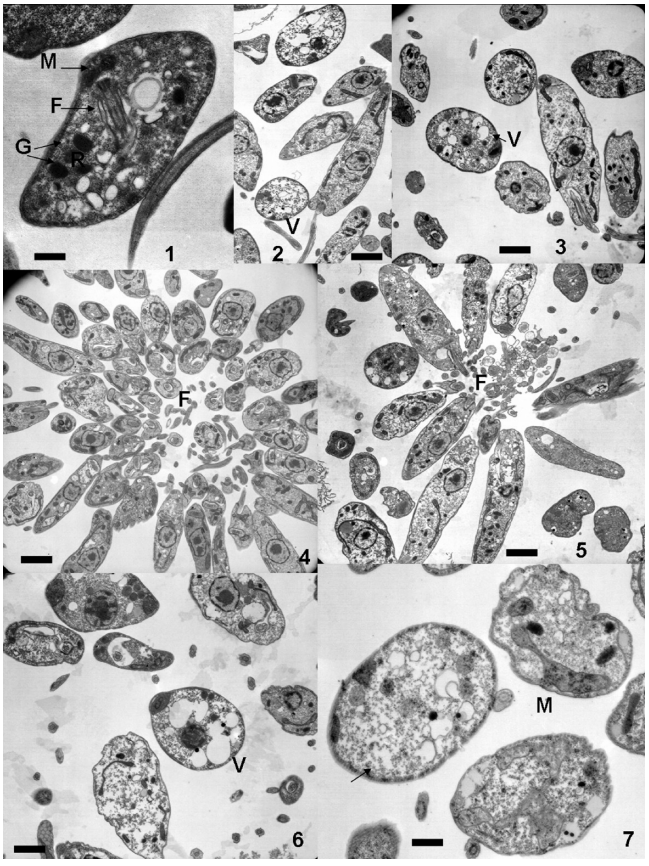

Figure 5. Ultrastructural alterations by TEM in *T. cruzi* treated with nickel(II) complexes (at IC_{25} concentration). (1) Control parasite showing organelles with their characteristic aspect, such as nucleus (N), mitochondrion (M), flagellum (F), vacuole (V). Bar = 0.583 μm. (2) Epimastigotes of *T. cruzi* treated with **3**. Bar = 2.33 μm. (3) Epimastigotes of *T. cruzi* treated with **4**. Bar = 1.59 μm. (4) Epimastigotes of *T. cruzi* treated with **9**. Bar = 2.33 μm. (5) Epimastigotes of *T. cruzi* treated with **8**. Bar = 2.33 μm. (6) Epimastigotes of *T. cruzi* treated with **7**. Bar = 1.59 μm. (7) Epimastigotes of *T. cruzi* treated with **6**. Bar = 1.35 μm.

normal morphology. Only a few of the epimastigote forms showed the cytoplasm full of empty vacuoles, as their unique ultrastructural alteration. **9** and **8** exerted an agglutinant effect over the epimastigote forms of *T. cruzi* (panel 4 of Figure 5 and panel 5 of Figure 5, respectively). In both cases, the epimastigote forms appeared forming rosettes. Ultrastructurally, the parasites showed a normal appearance, with the only exception that many flagella where found in the culture medium. This alteration was clearly stated in **8**, which at the same time produced a higher formation of vacuoles in the cytoplasm, so we may infer that **8** is slightly more effective than **9**. In the case of **7** (panel 6 of Figure 5), most of the epimastigote forms showed a strongly vacuolized cytoplasm, and a picnotic nucleus and a large number of free flagella could be observed in the supernatant, with a small proportion of dead parasites. Finally, **6** (panel 7 of Figure 5), one of the more effective products, induced many changes in the parasites: the cytoplasm appeared with granular aspect in most of them, was little electrodense, and was very vacuolized; some removed flagella were found in the supernatant; the mitochondria were swelled; and the nucleus was disorganized in some parasites.

3. Conclusions

Our results showed that six of the tested nickel complexes were very active in vitro against both extracellular and intracellular forms of *Trypanosoma cruzi* (in the order **8** > **3** ≥ **6** > **4** > **7** > **9**). These compounds are not toxic for the host cells and are effective at concentrations lower than the reference drug used in the present study (benznidazole). The in vitro growth rate of *T. cruzi* was reduced, its capacity to infect cells was negatively affected, and the multiplication of the amastigotes and subsequent transformation to trypomastigotes were greatly lowered. Moreover, a wide range of ultrastructural alterations in epimastigote forms of *T. cruzi* treated with these triazolopyrimidine complexes were found. These alterations, mainly at the mitochondria level, explain the metabolic changes in productions of succinate and acetate and may be due to the disturbance of the enzymes implied in the sugar metabolism inside the mitochondria. In vivo studies revealed results that were consistent with those observed in vitro. No sign of toxicity was observed in the treatment of mice with nickel complexes, and the parasitic charge was significantly lower than in the control assay with benznidazole. The effects of these products were also demonstrated with the anti *T. cruzi* antibody level modification during the chronic stage. In summary, a new family of antiparasitic agents, displaying promising in vivo activity, has been developed and deserves further study. The synthesis of new derivatives and preclinical studies, such as doses, schedule, strains, and toxicological studies, are currently in progress.

4. Experimental Section

4.1. Synthesis of the Compounds. The synthesis of 4,6-dimethyl-1,2,3-triazolo[4,5-*d*]pyrimidin-5,7-dione (Hdmax, **1**) was carried out according to the published method of Nübel and Pfleiderer,[32] while the synthesis of the corresponding sodium salt was described previously by us.[17] Other reagents were obtained form commercial sources and used without further purification. The synthesis of $Ni(dmax)_2 \cdot 6H_2O$ (**2**), $[Ni(dmax)_2(en)_2] \cdot 3H_2O$ (**3**), $Ni(dmax)_2(dap)_2 \cdot 1.5H_2O$ (**4**), and $Ni(dmax)_2(bapa) \cdot H_2O$ (**5**) has been previously reported.[17,18]

$[Ni(dmax)_2(phen)_2]$ (**6**) and $[Ni(phen)_3](dmax)_2 \cdot 7H_2O$ (**7**) complexes were obtained by mixing of 0.1 mmol of **2** dissolved in acetonitrile and the appropriate amount of 1,10-phenanthroline dissolved in ethanol (0.2 and 0.3 mmol for the synthesis of **6** and **7**, respectively). For both of them, the slow evaporation of these mixtures of solvents allowed the formation of pink crystals suitable for X-ray studies. **6**: Anal. Calcd for $C_{36}H_{28}N_{14}NiO_4$: C, 55.5; H, 3.6; N, 25.2. Found: C, 55.3; H, 4.1; N, 25.8%. **7**: Anal. Calcd for $C_{48}H_{50}N_{16}NiO_{11}$: C, 53.1; H, 4.6; N, 20.6. Found: C, 53.0; H, 4.7; N, 20.9%.

For the synthesis of $[Ni(dmax)_2(bpy)_2](H_2O)_{0.5}$ (**8**), 0.1 mmol of **2** and 0.2 mmol of 2,2′-bipyridyl were dissolved in 15 mL of methanol. The slow evaporation of the solvent allowed the formation of pink crystals suitable for X-ray studies. Anal. Calcd for $C_{32}H_{28}N_{14}NiO_4$: C, 51.9; H, 3.9; N, 26.5. Found: C, 52.2; H, 4.1; N, 26.6%.

For the synthesis of $Ni(dmax)_2(dpyamin)_2(H_2O)$ (**9**), 0.2 mmol of **2** and 0.6 mmol of 2,2′-dipyridylamine were each dissolved in 20 mL of acetonitrile. After both solutions were mixed, a mauve precipitate immediately appeared which was filtered off and washed with water and ethanol. Anal. Calcd for $C_{32}H_{32}N_{16}NiO_5$: C, 49.3; H, 4.1; N, 28.8. Found: C, 48.9; H, 4.3; N, 28.9%.

The elemental analysis results (including those for the previously reported compounds) are taken as a guarantee that the purity of the isolated compounds is higher than 95%.

4.2. Instrumentation. Microanalysis of C, H, and N were performed in a Fisons Instruments EA-1008 analyzer. Thermal

behavior was studied under an air flow in Shimadzu TGA-50 and Shimadzu DSC-50 equipment at heating rates of 20 and 10 °C min^{-1}, respectively. Reflectance diffuse spectra were made on a Varian model Cary-5E spectrophotometer, while magnetic susceptibility measurements, in the temperature range of 2−300 K, were carried out on powdered samples using a Quantum Design MPMS-XL SQUID using magnetic fields of 5×10^3 Oe. All this equipment is sited at the Centre of Scientific Instrumentation of the University of Granada, Spain. IR spectra were recorded on a ThermoNicolet IR 200 spectrometer using KBr pellets.

4.3. X-ray Crystallography. Data for **6**, **7**, and **8** were collected at room temperature in a Bruker SMART APEX CCD system with Mo Kα radiation (λ = 0.7107 Å). The structures were solved by the heavy atom method and anisotropically refined in F^2 using SHELXL-97.[33] Hydrogen atoms of the heterocycles were placed in ideal positions, whereas those of the water molecules were clearly spotted in the ΔF maps and refined with restrained O−H distance (0.84(1) Å), except for **7** where the hydrogen atoms of some water molecules could not be localized including those water molecules with partial occupation. Isotropic thermal parameters of all H atoms were fixed to 1.2 times the equivalent isotropic thermal parameter of their parent atoms. Table 1 summarizes the crystallographic data for these compounds.

4.4. Biological Tests. 4.4.1. Parasite Strain, Culture. The Maracay strain of *T. cruzi* was isolated at the Institute of Malariology and Environmental Health in Maracay (Venezuela). Epimastigote forms were obtained in biphasic blood-agar NNN medium (Novy−Nicolle−McNeal) supplemented with minimal essential medium (MEM) and 20% inactivated fetal bovine serum and afterward reseeded in a monophasic culture (MTL), following the method of Luque et al.[34]

4.4.2. In Vitro Trypanocidal Activity Assay. To obtain the parasite suspension for the trypanocidal assay, the epimastigote culture (in exponential growth phase) was concentrated by centrifugation at 1000*g* for 10 min and the number of flagellates were counted in an hemocytometric chamber and distributed into aliquots of 2×10^6 parasites/mL. The compounds were dissolved in DMSO (Panreac, Barcelona, Spain) at 0.01%, after being assayed as nontoxic and without inhibitory effects on the parasite growth. The compounds were dissolved in the culture medium, and the dosages used were 100, 50, 25, 10, and 1 μM. The effect of each compound against epimastigote forms, as well as the concentrations (assayed at different concentrations every drug), was evaluated at 72 h, using a Neubauer hemocytometric chamber.

4.4.3. Cell Culture and Cytotoxicity Tests. Vero cells (Flow) were grown in MEM (Gibco) supplemented with l0% inactivated fetal calf serum and adjusted to pH 7.2 in a humidified 95% air−5% CO_2 atmosphere at 37 °C for 2 days. For the cytotoxicity test, cells were placed in 25 mL colie-based bottles (Sterling), and centrifuged at 100*g* for 5 min. The culture medium was removed, and fresh medium was added to give a final concentration of 1×10^5 cells/mL. This cell suspension was distributed in a culture tray (with 24 wells) at a rate of 100 μL/well and incubated for 2 days at 37 °C in a humid atmosphere enriched with 5% CO_2. The medium was removed, and the fresh medium was added together with the product to be studied (at 100, 50, 25, l0, and 1 μM). The cultures were incubated for 72 h. The vital stain trypan blue (0.1% in phosphate buffer) was used to determine cell viability. The number of dead cells was recorded, and the percent viability was calculated in comparison to that of the control culture. The IC_{50} was calculated by linear regression analysis from the K_c values at the concentrations employed.

4.4.4. Transformation of Epimastigote to Metacyclic Forms. As a means of inducing metacyclogenesis, parasites were cultured at 28 °C in modified Grace's medium (Gibco) for 12 days as described previously.[35] Twelve days after cultivation at 28 °C, metacyclic forms were counted in order to infect Vero cells. The proportion of metacyclic forms was around 40% at this stage.

4.4.5. Cell Assay. Vero cells were cultured in MEM medium in a humidified 95% air−5% CO_2 atmosphere at 37 °C. Cells were seeded at a density of 1×10^5 cells/well in 24-well microplates (Nunc) with rounded coverslips on the bottom and cultivated for 2 days. Afterward, the cells were infected in vitro with metacyclic forms of *T. cruzi* at a ratio of 10:1. The drugs (IC_{25} concentrations) were added immediately after infection and were incubated for 6 h at 37 °C in a 5% CO_2 atmosphere. The nonphagocytized parasites and the drugs were removed by washing, and then the infected cultures were grown for 10 days in fresh medium. Fresh culture medium was added every 48 h.

The drug activity was determined from the percentage of infected cells and the number of amastigotes per cells infected in treated and untreated cultures in methanol-fixed and Giemsa-stained preparations. The percentage of infected cells and the mean number of amastigotes per infected cell were determined by analyzing more than 100 host cells distributed in randomly chosen microscopic fields. Values are the mean of four separate determinations. The number of trypomastigotes in the medium was determined as described previously.[35]

4.4.6. In Vivo Trypanocidal Activity Assay. Groups of five BALB/c female mice (6−8 weeks old, 25−30 g) maintained under standard conditions were infected with 1×10^3 bloodstream *T. cruzi* metacyclic forms by the intraperitoneal route. The animals were divided into the following groups: (i) group 1, uninfected (not infected and not treated); (ii) group 2, untreated (infected with *T. cruzi* but not treated); (iii) group 3, uninfected (not infected and treated with 1 mg/kg of body weight per day for 5 consecutive days (7−12 postinfection) by the intraperitoneal route);[27] (iv) group 4, treated (infected and treated for 5 consecutive days (7−12 postinfection) with the compounds and benznidazole).

Five days after infection, the presence of circulating parasites was confirmed by the microhematocrit method: an amount of 5 μL of blood drawn from the tail of the treated mice was taken and diluted 1:15 (50 μL of citrate buffer and 20 μL of lysis buffer at pH 7.2), and this vehicle was also employed as a negative control. The counting of parasites was done in a Neubauer chamber. The number of deaths was recorded every 2 days.

For serologic studies, one group of four animals treated with each compound and BZN was included. Treatments were started 7 days after animal infection. Compounds were administered in a similar way as that explained earlier and in the same concentration.

Quantitative evaluation of circulating anti *Trypanosoma cruzi* antibodies, at days 60 and 90 postinfection, was carried out by the use of an enzyme-linked immunoassay. The sera, diluted to 1:100, were reacted with an antigen constituted by a soluble Fe-SODe of *T. cruzi* epimastigotes. The results are expressed as the ratio of the absorbance (Abs) of each serum sample at 490 nm to the cutoff value. The cutoff for each reaction was the mean of the values determined for the negative controls plus 3 times the standard deviation.

4.4.7. Metabolite Excretion. Cultures of *T. cruzi* epimastigotes (initial concentration of 5×10^5 cells/mL) received IC_{25} of the compounds (except for control cultures). After incubation for 72 h at 28 °C, the cells were centrifuged at 400*g* for l0 min. The supernatants were collected to determine excreted metabolites by nuclear magnetic resonance spectroscopy (^{1}H NMR) as previously described by Fernández-Becerra et al.[36] The chemical displacements were expressed in parts per million (ppm), using sodium 2,2-dimethyl-2-silapentane-5-sulfonate as the reference signal. The chemical displacements used to identify the respective metabolites were consistent with those described by Fernández-Becerra et al.[36]

4.4.8. Ultrastructural Alterations. The parasites, at a density of 5×10^6 cells/mL, were cultured in their corresponding

medium, containing the drugs at the IC_{25} concentration. After 72 h, the cultures were centrifuged at 400*g* for 10 min and the pellets washed in PBS and then fixed with 2% (v/v) paraformaldehyde−glutaraldehyde in 0.05 M cacodylate buffer (pH 7.4) for 2 h at 4 °C. Pellets were prepared for transmission electron microscopy following the technique of Luque et al.[34]

Acknowledgment. This work was financially supported by MEC (Spain), Grant CGL2008-03687-E/BOS, and the Junta de Andalucía (Project P08-FQM-3705 and Research Group FQM195). C.R.M. is grateful for a FPU Grant from the Ministry of Education and Science of Spain.

Supporting Information Available: Crystallographic data for compounds **6**, **7**, and **8** (CCDC 765814, 765815, and 765813, respectively) in CIF format. This material is available free of charge via the Internet at http://pubs.acs.org.

References

(1) Pinto-Dias, J. C. The treatment of Chagas disease (South American trypanosomiasis). *Ann. Intern. Med.* **2006**, *144*, 772–774.
(2) Teixeira, A. R. L.; Nitz, N.; Guimaro, M. C.; Gomes, G.; Santos-Buch, C. A. Chagas disease. *Postgrad. Med. J.* **2006**, *82*, 788–798.
(3) Rocha, M. O. C.; Teixeira, M. M.; Ribeiro, A. L. An update on the management of Chagas cardiomyopathy. *Expert Rev. Anti-Infect. Ther.* **2007**, *5*, 727–743.
(4) Coura, J. R.; de Castro, S. L. A critical review on Chagas disease chemotherapy. *Mem. Inst. Oswaldo Cruz* **2002**, *97*, 3–24.
(5) Villa, L.; Morote, S.; Bernal, O.; Bulla, D.; Albajar-Vinas, P. Access to diagnosis and treatment of Chagas disease/infection in endemic and non-endemic countries in the XXI century. *Mem. Inst. Oswaldo Cruz* **2007**, *102*, 87–94.
(6) Docampo, R.; Moreno, S. N. Free radical metabolism of antiparasitic agents. *Fed. Proc.* **1986**, *45*, 2471–2476.
(7) Cerecetto, H.; González, M. Chemotherapy of Chagas' disease: status and new development. *Curr. Top. Med. Chem.* **2002**, *2*, 1187–1213.
(8) Braña, M. F.; Cacho, M.; García, M. L.; Mayoral, E. P.; López, B.; de Pascual-Teresa, B.; Ramos, A.; Acero, N.; Llinares, F.; Muñoz-Mingarro, D.; Lozach, O.; Meijer, L. Pyrazolo[3,4-*c*]pyridazines as novel and selective inhibitors of cyclin-dependent kinases. *J. Med. Chem.* **2005**, *48*, 6843–6854.
(9) Gangjee, A.; Lin, X.; Kisliuk, R. L.; McGuire, J. J. Synthesis of *N*-{4-[(2,4-diamino-5-methyl-4,7-dihydro-3*H*-pyrrolo[2,3-*d*]pyrimidin-6-yl)thio]benzoyl}-L-glutamic acid and *N*-{4-[(2-amino-4-oxo-5-methyl-4,7-dihydro-3*H*-pyrrolo[2,3-*d*]pyrimidin-6-yl)thio]-benzoyl}-L-glutamic acid as dual inhibitors of dihydrofolate reductase and thymidylate synthase and as potential antitumor agents. *J. Med. Chem.* **2005**, *48*, 7215–7222.
(10) Ballard, P.; Barlaam, B. C.; Bradbury, R. H.; Dishington, A.; Hennequin, L. F. A.; Hickinson, D. M.; Hollingsworth, I. M.; Kettle, J. G.; Klinowska, T.; Ogilvie, D. J.; Pearson, S. E.; Scott, J. S.; Suleman, A.; Whittaker, R.; Williams, E. J.; Wood, R.; Wright, L. Neutral 5-substituted 4-anilinoquinazolines as potent, orally active inhibitors of erbB2 receptor tyrosine kinase. *Bioorg. Med. Chem. Lett.* **2007**, *17*, 6326–6329.
(11) Urbina, J. A.; Docampo, R. Specific chemoterapy of Chagas disease: controversies and advances. *Trends Parasitol.* **2003**, *19*, 495–501.
(12) Magán, R.; Marín, C.; Rosales, M. J.; Salas, J. M.; Sánchez-Moreno, M. Therapeutic potential of new Pt(II) and Ru(III) triazole-pyrimidine complexes against *Leishmania donovani*. *Pharmacology* **2005**, *73*, 41–48.
(13) Boutaleb-Charki, S.; Marín, C.; Maldonado, C. R.; Rosales, M. J.; Urbano, J.; Gutiérrez-Sánchez, R.; Quirós, M.; Salas, J. M.; Sánchez-Moreno, M. Copper(II) complexes of [1,2,4]triazolo[1,5-*a*]-pyrimidine derivatives as potential antiparasitic agents. *Drug Metab. Lett.* **2009**, *3*, 35–44.
(14) Holý, A.; Dvořáková, H.; Jindřich, J.; Masojídková, M.; Budějšínský, M.; Balzarini, J.; Andrei, G.; Clercq, E. D. Acyclic nucleotide analogs derived from 8-azapurines: synthesis and antiviral activity. *J. Med. Chem.* **1996**, *39*, 4073–4088.
(15) Havlicek, L.; Fuksova, K.; Krystof, V.; Orsag, M.; Vojtesekd, B.; Strnadc, M. 8-Azapurines as new inhibitors of cyclin-dependent kinases. *Bioorg. Med. Chem.* **2005**, *13*, 5399–5407.
(16) Giorgi, I; Bianucci, A. M.; Biagi, G.; Livi, O.; Scartoni, V.; Leonardi, M.; Pietra, D.; Coi, A.; Massarelli, I.; Nofal, F. A.; Fiamingo, F. L.; Anastasi, P.; Giannini, G. Synthesis, biological activity and molecular modelling of new trisubstituted 8-azaadenines with high affinity for A1 adenosine receptors. *Eur. J. Med. Chem.* **2007**, *42*, 1–9.
(17) Maldonado, C. R.; Quirós, M.; Salas, J. M.; Rodríguez-Diéguez, A. A study of the second coordination sphere in 8-azaxanthinato salts of divalent metal aquacomplexes. *Inorg. Chim. Acta* **2009**, *362*, 1553–1558.
(18) Maldonado, C. R.; Quirós, M.; Salas, J. M. Ternary Ni(II) and Cu(II) complexes with 4,6-dimethyl-1,2,3-triazolo-[4,5-*d*]pyrimidin-5,7-dionato and chelating aliphatic amines as auxiliary ligands: variability in the binding site and hydrogen-bond networks. *Polyhedron* **2010**, *29*, 372–378.
(19) Dou, Y.-S. Equations for calculating *Dq* and *B*. *J. Chem. Educ.* **1990**, *67*, 134.
(20) Lever, A. B. P. *Inorganic Electronic Spectroscopy*; Studies in Physical and Theoretical Chemistry, 33; Elsevier Science Publishers B.V.: Amsterdam, 1984; ISBN 0-444-423893.
(21) Maldonado, C. R.; Quirós, M.; Salas, J. M. First and second coordination spheres in divalent metal compounds containing pyridine and 4,6-dimethyl-1,2,3-triazolo[4,5-*d*]pyrimidin-5,7-dione. *Polyhedron* **2009**, *28*, 911–916.
(22) Mabbs, F. E.; Machin, D. J. *Magnetism and Transition Metal Complexes*; Champman and Hall: London, 1973; ISBN 412-11230-2.
(23) Abdel-Rahman, L.; Battaglia, L. P.; Rizzoli, C.; Sgarabotto, P. Synthesis, characterization and X-ray crystal structure of tris(1,10-phenanthroline)nickel(II) perchlorate hemihydrate. *J. Chem. Crystallogr.* **1995**, *25*, 629–632.
(24) Singh, U. P.; Aggarwal, V. Hydrogen-bonding and $\pi-\pi$ stacking interactions in tris(1,10-phenanthroline-κ^2N,N')nickel(II) bis{[1-*tert*-butylimidazole-2(3*H*)-thione-κS]trichloridonickelate(II)} acetonitrile disolvate. *Acta Crystallogr.* **2008**, *E64*, m935–m936.
(25) Sánchez, M. P.; Romero, M. A.; Salas, J. M.; Cárdenas, D. J.; Molina, J.; Quirós, M. Molecular orbital study of 8-azaxanthine derivatives and crystal structure of 1,3-dimethyl-8-azaxanthine monohydrate. *J. Mol. Struct.* **1995**, *344*, 257–264.
(26) Porcal, W.; Hernández, P.; Aguirre, G.; Boiani, L.; Boiani, M.; Merlino, A.; Ferreira, A.; Di Maio, R.; Castro, A.; González, M.; Cerecetto, H. Second generation of 5-ethenylbenzofuroxan derivatives as inhibitors of *Trypanosoma cruzi* growth: synthesis, biological evaluation and structure−activity relationships. *Bioorg. Med. Chem.* **2007**, *15*, 2768–2781.
(27) González, P.; Marín, C.; Rodríguez-González, I.; Hitos, A. B.; Rosales, M. J.; Reina, M.; Díaz, J. G.; González-Coloma, A.; Sánchez-Moreno, M. In vitro activity of C_{20}-diterpenoid alkaloid derivatives in promastigotes and intracellular amastigotes of *Leishmania infantum*. *Int. J. Antimicrob. Agents* **2005**, *25*, 136–141.
(28) França da Silva, C.; Batista, M. M.; Batista, D. G. J.; Mello de Souza, E.; Bernardino da Silva, P.; Melo de Oliveira, G.; Meuser, A. S.; Shareef, A.-R.; Boykin, D. W.; Soeiro, M. N. C. In vitro and in vivo studies of the trypanocidal activity of a diarylthiophene diamidine against *Trypanosoma cruzi*. *Antimicrob. Agents Chemother.* **2008**, *52*, 3307–3314.
(29) de Souza, E. M.; Oliveira, G. M.; Soeiro, M. N. C. Electrocardiographic findings in acutely and chronically *T. cruzi*-infected mice treated by a phenyl-substituted analogue of furamidine DB569. *Drug Target Insights* **2007**, *2*, 61–69.
(30) Bringaud, F.; Rivière, L.; Coustou, V. Energy metabolism of trypanosomatids: adaptation to available carbon sources. *Mol. Biochem. Parasitol.* **2006**, *149*, 1–9.
(31) Ginger, M. L. Trypanosomatid biology and euglenozoan evolution: new insights and shifting paradigms revealed through genome sequencing. *Protist* **2005**, *156*, 377–392.
(32) Nubel, G.; Pfleiderer, W. Purine, V: Uber die synthese und struktur von 8-aza-xanthin (5.7-dioxo-tetrahydro-v-triazolo[4.5-*d*]pyrimidin) und seinen *N*-methyl-derivaten. *Chem. Ber.* **1965**, *98*, 1060–1072.
(33) Sheldrick, G. M. *SHELXL-97, Program Package for Solving and Refining Crystal Structures*; University of Göttingen: Göttingen, Germany, 1997.
(34) Luque, F.; Fernández-Ramos, C.; Entrala, E.; Rosales, M. J.; Navarro, J. A.; Romero, M. A.; Salas-Peregrín, J. M.; Sánchez-Moreno, M. In vitro evaluation of newly synthesised [1,2,4]-triazolo[1,5-*a*]pyrimidine derivatives against *Trypanosoma cruzi*, *Leishmania donovani* and *Phytomonas staheli*. *Comp. Biochem. Physiol.* **2000**, *126*, 39–44.
(35) Osuna, A.; Adroher, F. J.; Lupiañez, J. A. Influence of electrolytes and non-electrolytes on growth and differentiation of *Trypanosoma cruzi*. *Cell Differ. Dev.* **1990**, *30*, 89–95.
(36) Fernández-Becerra, C.; Sánchez-Moreno, M.; Osuna, A.; Opperdoes, F. R. Comparative aspects of energy metabolism in plant trypanosomatids. *J. Eukaryotic Microbiol.* **1997**, *44*, 523–529.